Proceedings of "Applications of Physics in Mechanical and Material Engineering" (APMME 2023)

Study of the Real Structure of Soft Magnetic Amorphous Alloys Using Mössbauer Spectroscopy

B. Jeż[a,*], M. Nabiałek[b], P. Pietrusiewicz[b], M.M. Nabiałek[b], A.V. Sandu[c,d] and T. Stachowiak[a]

[a] *Department of Technology and Automation, Faculty of Mechanical Engineering and Computer Science, Czestochowa University of Technology, al. Armii Krajowej 19c, 42-200 Częstochowa, Poland*
[b] *Department of Physics, Czestochowa University of Technology, al. Armii Krajowej 19, 42-200 Częstochowa, Poland*
[c] *Faculty of Materials Science and Engineering, Gheorghe Asachi Technical University of Iasi, Blvd. D. Mangeron 41, 700050, Iaşi, Romania*
[d] *Romanian Inventors Forum, Str. Sf. P. Movila 3, Iaşi, Romania*

Doi: 10.12693/APhysPolA.144.387 *e-mail: barlomiej.jez@pcz.pl

Studying the real structure of amorphous alloys is not an easy task and requires an appropriate scientific approach. Unlike crystalline materials, for which there is a precise description of the structure based on the structure of the unit cell, in amorphous materials it is not possible to identify it. The amorphous structure is often described as one big defect. Using the technique of Mössbauer spectroscopy, it is possible to study the structure of amorphous alloys and determine the degree of their order. The paper presents the results of Mössbauer tests for amorphous alloys in the state after solidification. The influence of a small change in the chemical composition on the probability of the occurrence of iron surroundings determining specific hyperfine field induction values was determined.

topics: bulk amorphous alloys, Mössbauer spectroscopy, X-ray diffraction (XRD)

1. Introduction

An important parameter indicating the application possibilities of various types of materials is their structure packing density. It is commonly understood as the number of closely packed atoms in a given volume, without distinguishing other relationships between atoms. In the case of ferromagnetic materials exhibiting magnetic properties, especially soft magnetic properties, the distribution of magnetic atoms in the volume of a given material is very important. The improvement in properties is not always related to a larger number of magnetic atoms in a given volume. A parameter that indirectly determines the good magnetic properties of magnetic alloys with soft magnetic properties is the exchange distance of magnetic interactions. This distance determines what distance between magnetic atoms is most favorable to obtain optimal properties described as ferromagnetic and soft magnetic [1, 2]. If this distance is too large, the magnetic interactions between atoms weaken and individual magnetic moments do not interact with each other. If there are too many of these atoms in the analyzed volume, their coupling occurs and the magnetic moments become antiparallel, and we are dealing with an antiferromagnetic interaction. Using Mössbauer transmission spectroscopy, and more precisely, numerical analysis of the obtained measurement results, it is possible to determine the distribution of iron atoms in the alloy volume. The hyperfine field induction distributions show low- and high-field components for amorphous alloys [3]. The change in magnetization was examined in the area where spin waves are thermally damped by the magnetic field and are responsible for its increase. The increase in magnetization in strong magnetic fields when it has almost been reached takes place according to the relationship describing the Holstein–Primakoff paraprocess [4]

$$b\left(\mu_0 H\right)^{1/2}, \tag{1}$$

where the coefficient b is described by the relationship

$$b = 3.54\, g\mu_0\mu_{\mathrm{B}} \left(\frac{1}{4\pi D_{spf}}\right)^{3/2} k_{\mathrm{B}} T \left(g\mu_B\right)^{1/2}, \tag{2}$$

and where:

k_{B} — Boltzmann constant,
μ_{B} — Bohr magneton,
g — gyromagnetic coefficient,
D_{spf} — spin wave stiffness parameter.

In (2), there is a spin wave stiffness parameter (D_{spf}), which is related to the exchange constant (A_{ex}) from the formula

$$A_{ex} = \frac{M_s D_{spf}}{2g\mu_{\mathrm{B}}}. \tag{3}$$

The spin wave stiffness parameter (D_{spf}) can be determined from the equation

$$D_{spf} = \frac{k}{4\pi}\left(\frac{2,612\mu_B\mu_0}{M_0 c_{3/2}}\right)^{3/2}, \tag{4}$$

where:

M_0 — magnetic polarization at 5 K,

$C_{3/2}$ — constant determined by adapting the law of the temperature dependence of magnetization as a function of the magnetic field strength ($\mu_0 H = 1$ T) [5].

Knowing the value of the spin wave stiffness parameter, we can determine the number of neighboring magnetic atoms.

The paper presents the results of tests of the structure and magnetic properties carried out for samples of $Fe_{62}Co_8Y_8Me_2B_{20}$ (Me = Nb or Zr) alloys in the form of ribbons after solidification and with a thickness of 35 μm.

2. Experimental procedure

The test material was prepared from ingredients with a purity of not less than 99.99 at.%. Four- and five-component alloys were made. The alloying base was iron, the content of which exceeded 60% for each alloy. This treatment prevents the loss of boron during remelting. Additionally, the alloys contained Co, Y, and Zr. After weighing 15 grams, the ingredients were pre-melted in an arc furnace. The alloy components were melted on a water-cooled copper plate. This process took place in a protective atmosphere of argon. The initial melting parameters are $\approx$ 250 A. After the first melting of the components, the operating current was increased to 350 A. Each subsequent melting of the ingot was performed after it had been rotated, which allowed for good mixing of the components. This operation was repeated twelve times. The melted alloy components in the form of an ingot were cooled in the furnace for about 15 min. This procedure was aimed at limiting the oxidation of the alloy. After being removed from the working furnace, the cooled ingots were cleaned mechanically and using an ultrasonic cleaner. The cleaned pieces of the alloy were ready to produce test samples in the form of thin ribbons. The ribbons were made using the melt-spinning method. The alloy pieces were placed in a quartz capillary, which was placed in the coil of an induction furnace. The capillary outlet had a diameter of 1 mm. The other side of the capillary was connected to an inert gas source. The copper wheel was accelerated to a linear speed of 30 m/s, and the liquid alloy was sprayed onto it. As a result, ribbons with a thickness of approximately 30–35 μm were produced. The ribbon production process was carried out in a protective atmosphere of argon. The ribbons thus produced were subjected to structure analysis using X-ray diffraction (XRD). An X-ray diffractometer operating in the Bragg–Brentano geometry was used for this purpose. The Bruker X-ray machine model ADVANCE 8 was equipped with an X-ray tube with a copper anode. Samples in the form of ribbons (planar-parallel) after solidification were glued to rotating measuring disks. Scanning of the ribbons using X-rays was carried out in the two theta angle range from 30 to 100°. The density and scanning time were 0.02° and 6 s, respectively. The spin wave stiffness parameter b was calculated based on the relationship from (1). Mössbauer spectra for room temperature were measured on a Polon 2330 spectrometer. The device operated in transmission geometry with constant source acceleration. The spectrometer calibration was performed on α-Fe foil with a thickness of 20 μm. A ^{57}Co Mössbauer source in a rhodium matrix was used for the measurements. The Mössbauer transmission spectra were subjected to numerical analysis using the NORMOS software [6].

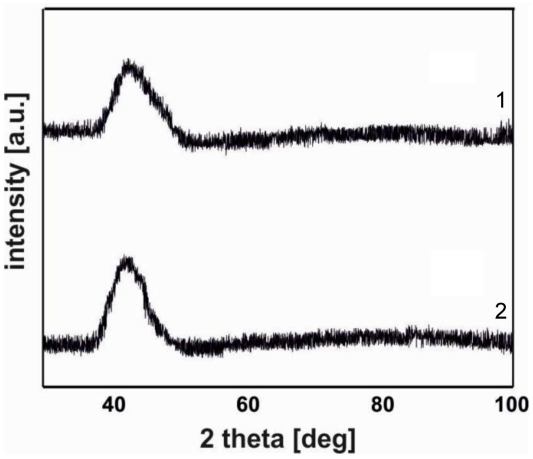

Fig. 1. X-ray diffraction images obtained for samples of the tested $Fe_{62}Co_8Y_8Me_2B_{20}$ in the form of 35 μm thick ribbons: with Zr (curve 1), and with Nb (curve 2).

3. Presentation of results

The X-ray diffractograms measured for the tested alloys are presented in Fig. 1.

The X-ray diffractograms for the tested alloys in the form of a ribbon presented in Fig. 1 are typical for materials with an amorphous structure. We can only distinguish a background of slight intensity. Near the two theta angles corresponding to the component with the highest content in the alloy (iron in our case), a wide diffuse maximum, called an amorphous halo, can be observed. The amorphous

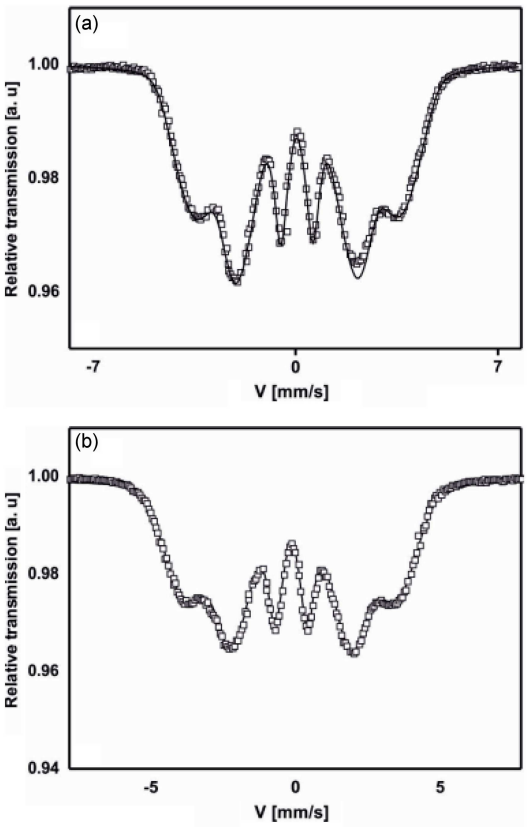

Fig. 2. Mössbauer transmission spectra obtained for the tested $Fe_{62}Co_8Y_8Me_2B_{20}$ in the form of 35 μm thick ribbons: (a) Zr, (b) Nb.

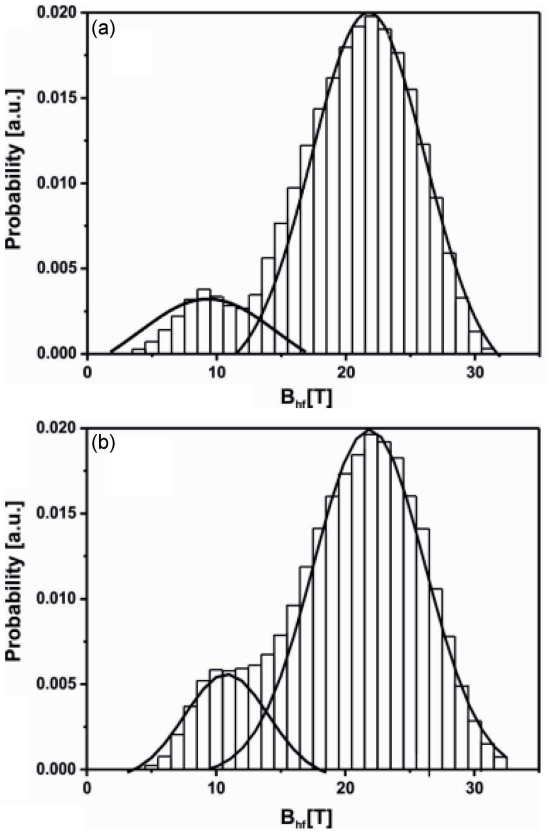

Fig. 3. Distributions of hyperfine field induction obtained based on the analysis of Mössbauer transmission spectra for the tested $Fe_{62}Co_8Y_8Me_2B_{20}$ in the form of 35 μm thick ribbons: (a) Zr, (b) Nb.

nature of the samples was additionally confirmed by tests performed using Mössbauer transmission spectroscopy. Figure 2 shows the Mössbauer transmission spectra obtained for the tested alloy samples.

The Mössbauer transmission spectra presented in Fig. 2 are typical for materials with an amorphous structure. They consist of wide asymmetrical overlapping lines and are asymmetrical. As a result of the numerical analysis of Mössbauer transmission spectra, the distributions of hyperfine field induction on ^{57}Fe nuclei were obtained (Fig. 3).

The distributions of hyperfine field induction on ^{57}Fe nuclei are bimodal. The low- and high-field components present in them indicate a large diversity of the immediate surroundings of iron atoms. This also means that in the volume of the alloy there are areas where the distances between iron atoms are smaller and areas where the distances are larger. The formation of such areas affects the occurrence of topological and chemical disorders in amorphous materials. This can be considered to be the nature of amorphous materials, which distinguishes them from crystalline materials. Figure 4 shows the dependencies $b(\mu_0 H)^{1/2}$ for the tested $Fe_{62}Co_8Y_8Me_2B_{20}$ in the form of 35 μm thick ribbons with Zr (curve 1) and Nb (curve 2).

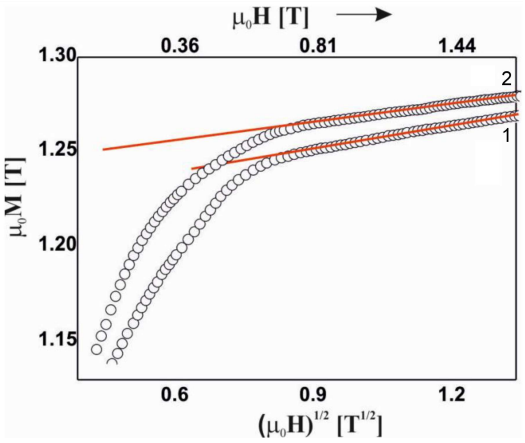

Fig. 4. The relationship $b(\mu_0 H)^{1/2}$ for the tested $Fe_{62}Co_8Y_8Me_2B_{20}$ alloys in the form of 35 μm thick ribbons: Nb (curve 1), Zr (curve 2).

The calculated spin wave stiffness parameter D_{spf} for the sample with the addition of Nb (61.8×10^{-2} meV nm^2) is higher than for the sample with Zr (56.4×10^{-2} meV nm^2). This may mean that in the alloy with the addition of Nb, the distances between magnetic atoms are more favorable for free interaction between magnetic spins.

4. Conclusions

The produced ribbons had an amorphous structure, which was confirmed by tests performed using XRD and Mössbauer spectroscopy. The distributions of hyperfine field induction on ^{57}Fe are bimodal, which is related to the presence of areas with different iron concentrations in the sample volume. In the sample with Nb addition, the average value of the hyperfine field of the low-field component was much higher. The increase in the value of the material parameter D_{spf} is related to the change in the internal parameters of the sample. As a result of a slight change in the composition of the alloy, the distance between the nearest magnetic neighboring atoms changes. The increase in the value of the D_{spf} parameter may be related to the increased number of closest magnetic atoms, which is related to the improvement of the short-range chemical order (SRO).

References

[1] M.-N. Avettand-Fenoel, M. Marinova, R. Taillard, W. Jiang, *J. Alloys Compd.* **854**, 157068 (2021).

[2] B. Jeż, M. Nabiałek, K. Jeż, *Acta Phys. Pol. A* **142**, 14 (2022).

[3] B. Jeż, J. Wysłocki, S. Walters, P. Postawa, M. Nabiałek, *Materials* **13**, 1367 (2020).

[4] T. Holstein, H. Primakoff, *Phys. Rev.* **58**, 1098 (1940).

[5] M. Hirscher, R. Reisser, R. Wurschum, H.E. Schaefer, H. Kronmüller, *J. Magn. Magn. Mater.* **146**, 117 (1995).

[6] R.A. Brand, NORMOS-90, Universität Duisburg, 2002.